

# Energy-rate consideration in wafer bonding

H. Fan<sup>a</sup>, J. G. Xu<sup>a</sup>, K.Y. Sze<sup>b,\*</sup>

<sup>a</sup>*School of Mechanical and Production Engineering, Nanyang Technological University, Singapore 639798, Singapore*

<sup>b</sup>*Department of Mechanical Engineering, University of Hong Kong, Hong Kong, PR China*

Received 30 April 2005; received in revised form 22 August 2005; accepted 30 October 2005

Available online 13 December 2005

## Abstract

In the present study, we consider the bonding process of a pair of wafers with rough surfaces via an energy-rate concept in which “rate” refers to “area rate”. A finite element numerical simulation for a rough surface with periodical distributed asperities bonded onto a rigid half-space is carried out for demonstrating the energy-rate concept. The simulation reveals various phenomena in the wafer bonding, such as self-activated bonding, asperity shape effect and plastic deformation effect in the bonding process.

© 2005 Elsevier B.V. All rights reserved.

*Keywords:* Wafer bonding; Contact mechanics; Energy rate; Finite element analysis

## 1. Introduction

Wafer-bonding technology has been widely applied in assembly of micro-systems. With this technology, two free surfaces of mirror polished, flat and clean solids of almost any material, are locally bonded together to form a cohesive interface spontaneously as shown in Fig. 1, leading to electronic and opto-electronic devices of much superior performance [1–5]. The micro-mechanism of wafer bonding comes from the short-range intermolecular and interatomic attraction forces, such as van der Waals forces, which are one or two orders of magnitude lower than typical values for covalent bonding [3,4]. In macroscopic viewpoint, this phenomenon can be explained by the reduction of surface energy after bonding. When two surfaces join to form an interface, the net free energy reduces. The reduction of energy per unit area, known as the work of adhesion, is

$$\Gamma = \gamma_1 + \gamma_2 - \gamma_{12}, \quad (1.1)$$

where  $\gamma_1$  and  $\gamma_2$  are the surface tensions of two wafer materials, respectively, and  $\gamma_{12}$  is the interface tension.

Yu and Suo [6] applied an energy criterion to the wafer bonding, which is read as

$$\Gamma A_{\text{total}} > U_{\text{total}}, \quad (1.2)$$

where  $A_{\text{total}}$  is the total interface area and  $U_{\text{total}}$  is the total strain energy installed in the bi-material after the external force is removed. They only examined complete bonding of two wavy surface wafers where they presented results in analytical form. It is noticed that this energy criterion, based on a comparison of the difference between the total energy before and after bonding, may not be able to examine certain phenomena, such as self-activated bonding, external loading assisted bonding, during the wafer-bonding process. In other words, Eq. (1.2) only stated the final state without any information on the bonding “history”.

In the following sections, we revisit the wafer-bonding process of rough surfaces via an energy-rate concept. A new criterion based on energy absorption rate (*energy absorption rate criterion*) is proposed in Section 2. It is remarked that “rate” here refers to “area rate” but not “time rate”. In Section 3, a finite element simulation for the bonding between a surface with sinusoidal profile and a flat half-space is carried out for demonstration of the new criterion. Parametric studies on asperity shape and plasticity in Section 5 are presented as the extensive understanding via the finite element simulation. The employed mesh has been checked to ensure adequate convergence.

\* Corresponding author. Tel.: +852 2859 2637; fax: +852 2858 5415.  
E-mail address: [kysze@hku.hk](mailto:kysze@hku.hk) (K.Y. Sze).

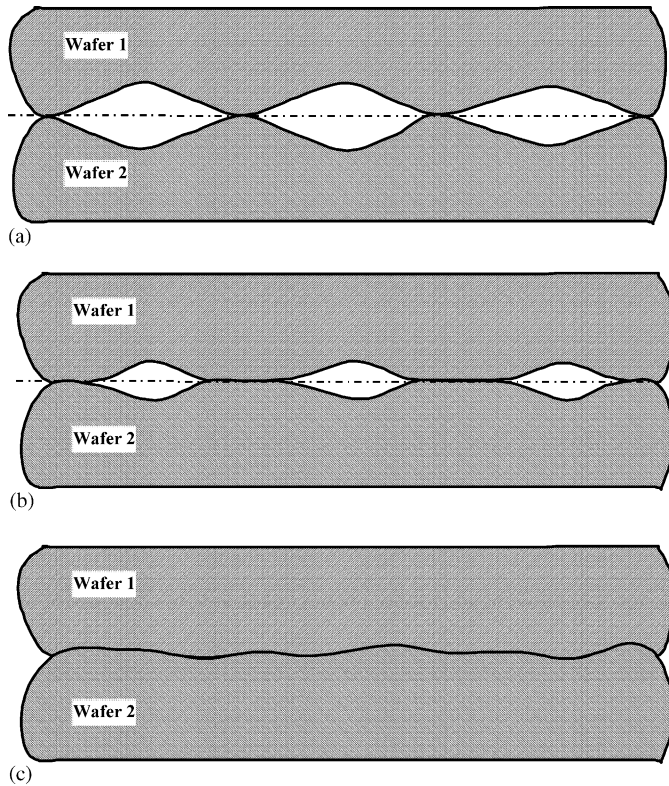


Fig. 1. Schematics of wafer bonding: (a) initial contact (b) partial bonding (c) complete bonding.

## 2. Energy absorption rate consideration in wafer bonding

For wafers to be bonded at room temperature, the misfit gap between the wafers must be accommodated by elastic or elasto-plastic deformation. Fig. 1 illustrates this bonding process. Prior to contact, two wafers are not perfectly flat. Once brought together, they contact at a few points first (Fig. 1(a)). In this state, the total free surface area is large, and so is the free energy. To reduce the free energy, the wafers deform elastically or elasto-plastically and transform the free surfaces into an interface. If the misfit is large, the wafers absorb more energy (the resistance to bonding is large), and the wafers are bonded only over patches of the surface area, leaving the rest of the area un-bonded (Fig. 1(b)). If the misfit is small, the wafers absorb less energy (the resistance to bonding is small), the wafers are bonded over the entire area (Fig. 1(c)).

In a quasi-static process of wafer bonding with external loading, for an infinitesimal increase of the interface area  $\delta A$ , the reduction of surfaces energies  $(\gamma_1 + \gamma_2)\delta A$ , the increase of interface energy  $\gamma_{12}\delta A$ , the work done by external loading  $\delta W$ , and strain energy  $\delta U$  which is generated near interface owing to mismatch of geometric configuration and material properties between two wafers, satisfy the following equation:

$$(\gamma_1 + \gamma_2 - \gamma_{12})\delta A + \delta W - \delta U = \Gamma\delta A - \delta(U - W) \geq 0. \quad (2.1)$$

It is straightforward to identify that the *driving force* to increase the interface area is  $\Gamma$  and the *resistance* to form the interface is

$$R = \frac{\partial(U - W)}{\partial A}. \quad (2.2)$$

$R$  is the *energy absorption rate* that represents the energy absorbed from the surface energy in forming unit area of the interface. This concept can be applied for either elastic or elastic–plastic deformations.

With the definition of resistance, Eq. (2.2), bonding is possible when

$$\Gamma \geq R. \quad (2.3)$$

Eq. (2.3) is hereafter called *energy absorption rate criterion*. Apparently, the energy absorption rate criterion indicates the following three possibilities.

(1) *Bonding process*: If the driving force  $\Gamma$  is larger than the resistance  $R$ , the system tends to reduce the energy by forming the interface.

(2) *Debonding process*: If the driving force  $\Gamma$  is smaller than the resistance  $R$ , the system tends to reduce the energy by breaking the interface to two separated surfaces.

(3) *An equilibrium state*: If the driving force  $\Gamma$  has the same value as the resistance  $R$ , an external load is needed to proceed either bonding or debonding.

It is noticed that integration of Eq. (2.1) with respect to the area  $A$  leads to Eq. (1.2), which has the same form as the total energy difference criterion.

$$\Gamma A > U. \quad (2.4)$$

As a demonstration of the energy-rate consideration, we carry out a finite element simulation numerical for a wafer-bonding process as follows.

## 3. A finite element simulation for bonding between elastic wavy surfaces

As mentioned in the previous section, the driving force for the wafer bonding ( $\Gamma$ ) is completely determined by the material properties, while the resistance ( $R$ ) is associated with the shape of the two surfaces and the external loading. The relationship between them is the key in the process of wafer bonding. Yu and Suo [6] obtained an analytical solution for a two-dimension periodic surface, in which only the complete bonding was considered based on energy balance concept or Eq. (1.2). When the partial bonding process is considered, where no analytical solution is available, a finite element analysis for the whole bonding process must be carried out.

Let us look at the following configuration for the finite element simulation. In the frictionless contact between two elastic solids, the contact stresses depend only upon the relative profile of the bodies in contact. Therefore, the system can be replaced by a flat rigid surface in contact with a body (having an effective modulus  $E^*$ , where  $1/E^* = (1 - \nu_1^2)/E_1 + (1 - \nu_2^2)/E_2$ , and a yielding stress  $\sigma_s$ ) and a profile that results in the same un-deformed gap between the surfaces. With this in our mind,

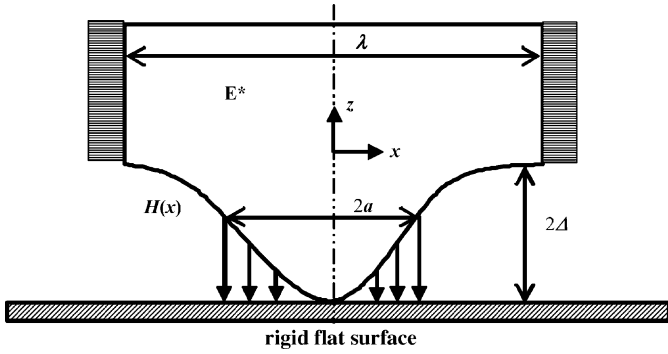


Fig. 2. The configuration used in FEA calculation.

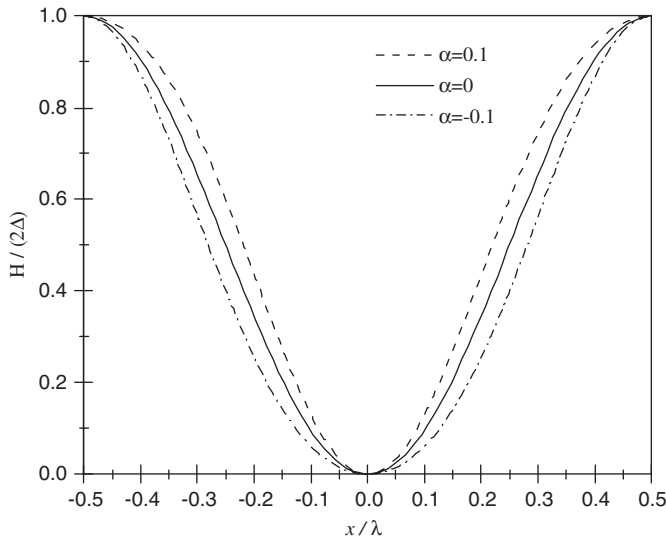


Fig. 3. Shapes of wavy surfaces with different  $\alpha$ .

we consider the bonding between a wavy surface with periodic profile and a rigid flat surface as shown in Fig. 2. The profile of the wavy surface is described by

$$H(x) = 2\Delta \left[ \sin^2\left(\frac{\pi x}{\lambda}\right) + \alpha \sin^2\left(\frac{2\pi x}{\lambda}\right) \right], \quad (3.1)$$

where  $\lambda$  is the wavelength, and  $2\Delta$  is the amplitude. The parameter  $\alpha$  is introduced to investigate the effects of the asperity shape on wafer bonding, which will be discussed in Section 5. The shape of the asperity for different  $\alpha$  is shown in Fig. 3.

Owing to the periodicity, we only considered one wavelength as shown in Fig. 2. Along the left and right boundaries, the periodic constraints are applied, i.e.  $u_x$  are same at  $x = \pm\lambda/2$ . The commercial finite element package ANSYS was employed to carry out the elastic/elastoplastic numerical calculation. In our finite element model, the wafer thickness, i.e. the dimension along the  $z$ -direction, is taken to be 10 times of  $\lambda$  so that effect of the contact between the wafer and the rigid plane on the stress field far from the contact interface can be ignored. Owing to symmetry, only half of the problem domain ( $x \geq 0$ ) is modeled. The finite element mesh is finest at the wavy surface and coarsest at the far end. From  $x=0$  to  $\lambda/2$  along the surface,

there are 50 elements which are all essentially squares in shape. The PLANE42 four-node incompatible element model of ANSYS is employed. To calculate the resistance of wafer bonding for different contact width  $2a$ , displacement constraints are first introduced such that the boundary node at  $x=0$  is brought into contact with the rigid base plate. In each incremental loading step, one additional displacement constraint is activated to bring the boundary node closest to the constrained boundary nodes into contact with the rigid base plate.

For a given contact width  $2a$ , the field of displacements, strains and stresses are calculated.  $U$  is computed by summation of the strain energy over all elements in the problem domain. In turn, the resistance  $R$ , defined by Eq. (2.2), is calculated according to

$$R(2a) = \frac{\partial(U - W)}{\partial(2a)}. \quad (3.2)$$

For the present elastic–plastic boundary value problem, the following geometrical and physical quantities are taken in our parametric study.

- (i) The geometrical dimensions:  $\lambda$  (asperity wavelength is taken as 2 mm),  $\Delta$  (asperity amplitude),  $\alpha$  (indicating the asperity shape),  $a$  (half contact width);
- (ii) The material properties:  $E$  (Young’s modulus is taken as 50 GPa),  $\nu$  (Poisson’s ratio is taken as 0.3),  $\sigma_s$  (yielding stress) of the wafer.

In the elastoplastic calculation, the material is assumed to be elastic–perfectly-plastic. The von Mises yield criterion is adopted.

Dimensional analysis showed that there are four independent dimensionless groups in this problem. They are  $\Delta/\lambda$ ,  $\sigma_s\lambda/E^*\Delta$ ,  $\alpha$ ,  $2a/\lambda$ . Among these dimensionless parameters, we firstly take a look at the influence of  $\Delta/\lambda$  by numerically trying various value of this ratio. Numerical results show that the stress and strain in the wafer are proportional to  $E^*\Delta/\lambda$  and  $\Delta/\lambda$ , respectively, and the density of strain energy is proportional to  $E^*(\Delta/\lambda)^2$ . In all our presentation, we take the average strain energy over the wavelength, which is defined by  $\bar{U} = U/\lambda$  in the wafer of unit thickness. If this energy is normalized by

$$R^* = \frac{\pi E^* \Delta^2}{2 \lambda}, \quad (3.3)$$

we find that different  $\Delta/\lambda$  values do not affect our results presented in Figs. 4–8.  $\sigma_s\lambda/E^*\Delta$  and  $\alpha$  will be discussed in Section 5.

The finite element numerical results shown in Fig. 4 quantitatively indicate the variation of  $\bar{U}$  and  $R$  with respect to  $2a/\lambda$ . The important and detailed features in Fig. 4 are: (1) the resistance  $R=0$  when the contact area equals to zero ( $a=0$ ), (2) The resistance  $R$  increases as the contact area increases and reaches its maximum value  $R_m = 1.02R^*$  at  $2a_m/\lambda = 0.68$ , (3) The resistance decreases to zero when the interface is completely bonded.

Our finite element numerical results are verified by the solution in the complete bonding of the elastic wafer with which

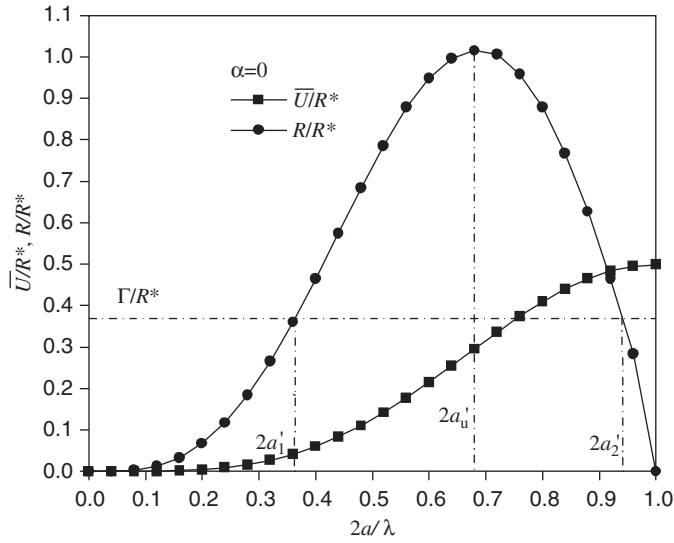


Fig. 4. Normalized strain energy and energy absorption rate vs. normalized contact area.

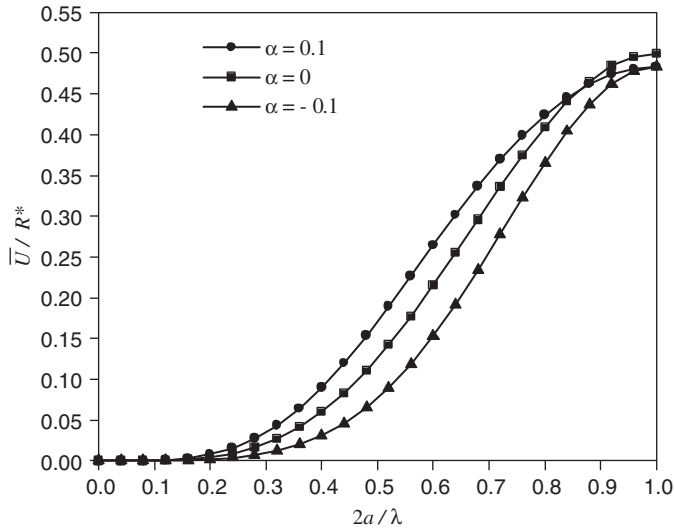


Fig. 5. Variation of normalized average strain energy vs. contact area with different  $\alpha$ .

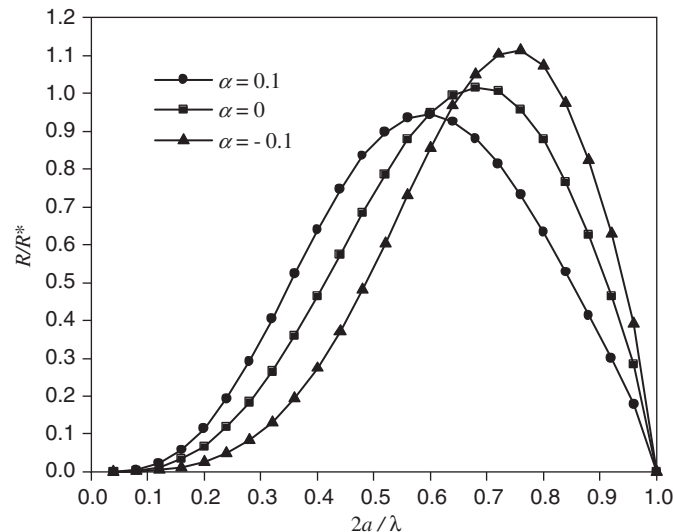


Fig. 6. Variation of resistance vs. contact area with different  $\alpha$ .

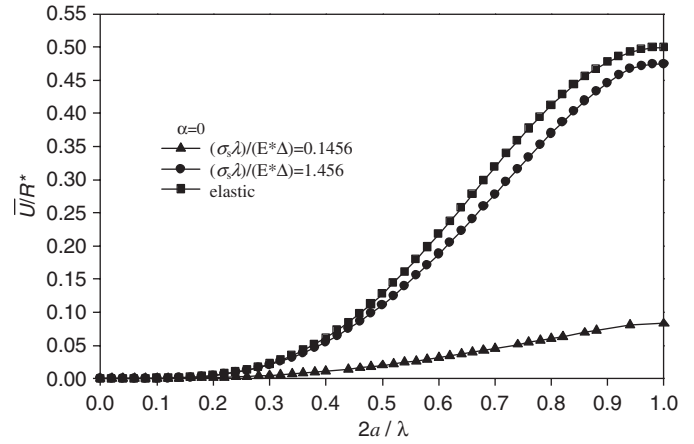


Fig. 7. Normalized strain energy vs. normalized contact area for elastoplastic deformation.

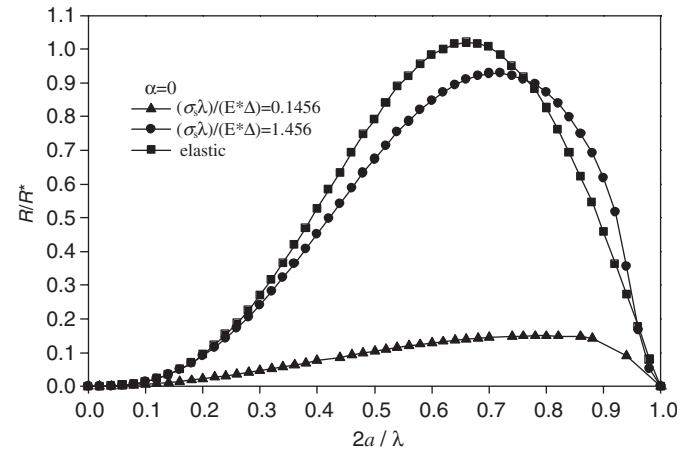


Fig. 8. Variation of resistance with contact area for different yielding stresses.

analytical solution is available. The numerical results of the strain energy and the maximum normal stress on the interface are compared with the corresponding analytical counterparts presented by Yu and Suo [6]. It is shown that our mesh produced results accurate enough to be used in the discussion of the wafer-bonding process.

#### 4. Self-activated and external loading assisted wafer bonding

When the far fields of the wafers are free of external loading, the wafers are only bonded due to the work of adhesion, which is called self-activated wafer bonding hereafter. The dimensionless strain energy and resistance are presented as functions of the contact area  $2a/\lambda$  in Fig. 4 where only elastic wafers with a surface profile of  $\alpha = 0$  are considered. In this section, with the finite element results in Fig. 4, we have quantitative description on various bonding phenomena by using the energy absorption rate criterion.

#### 4.1. Self-activated complete bonding

According to the energy-rate consideration, when the driving force  $\Gamma$  is greater than the maximum resistance  $1.02R^*$  (refer Fig. 4), the wafer bonding is self-activated without any external loading. For this case,

$$\frac{\Gamma\lambda}{E^*\Delta^2} > 1.60 \quad \text{or} \quad \Gamma/R^* > 1.02. \quad (4.1)$$

The strain energy in the wafer is  $\bar{U}(1)/R^* = 0.50$ .

In order to have a qualitative description to the bonding strength of the bonded interface, the *specific effective bonding energy*,  $E_b$ , which is the external mechanical work needed for separating per unit nominal area of contact interface, is introduced as follows:

$$E_b = \Gamma - \bar{U}(1). \quad (4.2)$$

Therefore, for the self-activated complete bonding, we have

$$E_b = \Gamma - \bar{U}(1) > (1.02 - 0.50)R^* = 0.52R^*. \quad (4.3)$$

It is seen that the interface is stronger with higher  $\Gamma$ .

#### 4.2. Self-activated partial bonding

When  $\Gamma$  is less than the maximum resistance  $1.02R^*$ , only partial bonding can be reached via the self-activated mechanism. The contact area is determined by

$$R(2a') = \Gamma. \quad (4.4)$$

where  $a' = a/\lambda$ . From Fig. 4, it can be seen that there are two solutions to this condition. They are denoted by  $2a'_1$  and  $2a'_2$  ( $a'_1 < a'_2$ ), respectively. Only the smaller,  $2a'_1$ , can be reached by self-activated mechanism. Further bonding is possible with help of some external loading.

For this partially bonded interface, the specific effective bonding energy is given by

$$E_b = 2a'_1\Gamma - \bar{U}(2a'_1). \quad (4.5)$$

#### 4.3. External loading assisted bonding and total energy difference criterion

External loading can be introduced via far-field pressure. As the magnitude of the pressure is arbitrary, the external loading assisted bonding process is not unique. We did a numerical simulation on wafer bonding with the presence of the external pressure. The function of the external pressure is to reduce the resistant level below the driving force  $\Gamma$  so that the condition Eq. (2.3) can be satisfied.

In this conjecture, we need to clarify the difference between “bonding” and “in contact” of two wafers. The “bonding” means that interface keeps unchanged after the external loading is withdrawn, while the “in contact” means that two wafers are pushed in contact by the external pressure but will separate after the external pressure is withdrawn. With these clarifications in our mind, we can understand that two wafers can be pushed

by external pressure into full range contact even for the case presented in Fig. 4 where complete bonding is not allowed by energy consideration.

It is now clear to us that energy consideration and energy-rate consideration are complementary. The former only stated the final states of the wafers’ bonding, while the “history” is not under its consideration. The statement is independent of external loading. On the other hand, the energy-rate consideration only focuses on the possibility of making two surfaces into “contact” with or without external loading. Apparently, we need both considerations to have the whole picture of the wafer bonding.

### 5. Effects of asperity shape and plasticity on wafer bonding

There are other important parameters affecting the process of the wafer bonding. Among the many parameters, we would like to discuss the following two geometric and material factors, namely, the asperity shape of the surface and plastic deformation of the wafers.

#### 5.1. Effects of the shape of asperity

For examining the changes of the asperity shape, we introduced various  $\alpha$  values in Eq. (3.1). Fig. 3 shows a blunter (smaller  $\alpha$ ) and a sharper (larger  $\alpha$ ) asperities. Figs. 5 and 6 show that even with the same wavelength and the same height, the asperity shape on the surface plays a role in the process of the wafer bonding. In Fig. 5, the strain energy for a surface with sharper asperities is larger than that for blunter in the partial bonding process. Nevertheless, when the complete bonding is concerned, the difference reduces and the values of the strain energies are very close to each other for different asperity shapes. On the other hand, the asperity shape affects the maximum resistance of wafer bonding significantly as shown in Fig. 6. The maximum resistance is larger for a surface with blunter asperities. Therefore, it is harder to bond wafers with blunter asperities. These indications should be meaningful even for randomly distributed rough surface, although the current simulation is carried out for a periodical distributed rough surface.

#### 5.2. Effects of plastic deformation

Plastic deformation occurs for the materials with low yielding stress. It is intuitive thinking that the soft materials (low yielding stress) provide low resistance to the bonding. The quantitative consideration is given in Figs. 7 and 8 where  $(\sigma_s\lambda/E^*\Delta)$  is taken as a dimensionless parameter that describes the level of the yielding in our data presentation. In Figs. 7 and 8, three curves are shown for various deformation situations. For elastic deformation, the  $(\sigma_s\lambda/E^*\Delta)$ -value is infinitely large. With  $E^*$  taken to be 50 GPa in Section 3, we further take  $\lambda/\Delta = 400$  and consider both  $\sigma_s = 200$  and 20 MPa. The former and latter stresses lead to mild and deep plastic deformation whereas their  $(\sigma_s\lambda/E^*\Delta)$ -values are 1.456 and 0.1456, respectively. The

quantitative study shown in Figs. 7 and 8 confirmed our intuitive concept that the low yielding stress materials are much easier to be bonded as both the resistance and strain energy are low.

## 6. Concluding remarks

In the present numerical study, we considered the wafer-bonding process via an energy absorption rate concept together with the existing energy-based criterion. Two concepts are complementary. The energy criterion predicts possible bonded area based on the wafer materials' constant and surface/interface properties. The energy-rate concept guides the process of putting two surfaces into contact and whether the external loading is needed for the process. Although the present numerical simulation is carried out for a periodical distributed asperity configuration, the concepts and conclusion made in the present paper shade some light on the random distributed rough surfaces.

## Acknowledgement

Discussion with Dr. Wang G.F. during the research of the present project is greatly appreciated.

## References

- [1] Z.L. Liao, Strained interface of lattice-mismatched wafer fusion, *Phys. Rev. B* 55 (19) (1997) 12899–12901.
- [2] U. Gösele, H. Stenzel, T. Martini, J. Steinkirchner, D. Conrad, K. Scheerschmidt, Self-propagating room-temperature silicon wafer bonding in ultrahigh vacuum, *Appl. Phys. Lett.* 67 (24) (1995) 3614–3616.
- [3] U. Gösele, Q.-Y. Tong, A. Schumacher, G. Kräuter, M. Reiche, A. Plöchl, P. Kopperschmidt, T.-H. Lee, W.-J. Kim, Wafer bonding for microsystems technologies, *Sensors Actuators A* 74 (1999) 161–168.
- [4] Q.-Y. Tong, U. Gösele, Semiconductor wafer bonding: recent developments, *Mater. Chem. Phys.* 37 (1994) 101–127.
- [5] C. Gui, M. Elwenspoek, N. Tas, J.G.E. Gardeniers, The effect of surface roughness on direct wafer bonding, *J. Appl. Phys.* 85 (10) (1999) 7448–7454.
- [6] H.H. Yu, Z. Suo, A model for wafer bonding by elastic accommodation, *J. Mech. Phys. Solids* 46 (5) (1998) 829–844.